Focusing polycapillary to reduce parasitic scattering for inelastic x-ray measurements at high pressure

P. Chow, Y. M. Xiao, E. Rod, L. G. Bai, G. Y. Shen, S. Sinogeikin, N. Gao, Y. Ding, and H.-K. Mao

---

Articles you may be interested in

The simultaneous measurement of energy and linear polarization of the scattered radiation in resonant inelastic soft x-ray scattering
Rev. Sci. Instrum. **85**, 115104 (2014); 10.1063/1.4900959

Application of a new composite cubic-boron nitride gasket assembly for high pressure inelastic x-ray scattering studies of carbon related materials
Rev. Sci. Instrum. **82**, 073902 (2011); 10.1063/1.3607994

Energy calibration of a high-resolution inelastic x-ray scattering spectrometer
Rev. Sci. Instrum. **79**, 083902 (2008); 10.1063/1.2968118

A pressure cell for nonresonant inelastic x-ray scattering studies of gas phases
Rev. Sci. Instrum. **79**, 086101 (2008); 10.1063/1.2964106

Novel rhenium gasket design for nuclear resonant inelastic x-ray scattering at high pressure
Rev. Sci. Instrum. **79**, 023903 (2008); 10.1063/1.2840772

HPSTAR
0114-2015

Focusing polycapillary to reduce parasitic scattering for inelastic x-ray measurements at high pressure

P. Chow,[1,a)] Y. M. Xiao,[1] E. Rod,[1] L. G. Bai,[1] G. Y. Shen,[1] S. Sinogeikin,[1] N. Gao,[2] Y. Ding,[3] and H.-K. Mao[4]

[1]HPCAT, Geophysical Laboratory, Carnegie Institution of Washington, 9700 South Cass Avenue, Argonne, Illinois 60439, USA
[2]Center for X-Ray Optics, University at Albany, State University of New York, 1400 Washington Avenue, Albany, New York 12222, USA and X-Ray Optical Systems, Inc., 90 Fuller Road, Albany, New York 12205, USA
[3]Advanced Photon Source, Argonne National Laboratory, Argonne, Illinois 60439, USA
[4]Geophysical Laboratory, Carnegie Institution of Washington, 5251 Broad Branch Road NW, Washington, District of Columbia 20015, USA

The double-differential scattering cross-section for the inelastic scattering of x-ray photons from electrons is typically orders of magnitude smaller than that of elastic scattering. With samples 10-100 μm size in a diamond anvil cell at high pressure, the inelastic x-ray scattering signals from samples are obscured by scattering from the cell gasket and diamonds. One major experimental challenge is to measure a clean inelastic signal from the sample in a diamond anvil cell. Among the many strategies for doing this, we have used a focusing polycapillary as a post-sample optic, which allows essentially only scattered photons within its input field of view to be refocused and transmitted to the backscattering energy analyzer of the spectrometer. We describe the modified inelastic x-ray spectrometer and its alignment. With a focused incident beam which matches the sample size and the field of view of polycapillary, at relatively large scattering angles, the polycapillary effectively reduces parasitic scattering from the diamond anvil cell gasket and diamonds. Raw data collected from the helium exciton measured by x-ray inelastic scattering at high pressure using the polycapillary method are compared with those using conventional post-sample slit collimation. © 2015 AIP Publishing LLC. [http://dx.doi.org/10.1063/1.4926890]

I. INTRODUCTION

When hard x rays impinge on a system of electrons, a variety of responses can occur. We focus here on inelastic x-ray scattering, in which the x-ray photon exchanges energy and momentum with electrons in the sample under study. The double differential cross-section is measured, which yields the dynamic structure factor S($\mathbf{q}$, ω).[1–4] The technique measures the energy loss of the x-ray photon ω, as a function of the momentum transfer of the photon, $\mathbf{q}$. When bonding states of the system are to be studied, and the photon energy loss is on the order of the binding energy of the electrons of interest, the technique is called x-ray Raman scattering. Under certain circumstances, x-ray Raman scattering yields the same information as x-ray absorption.[5] Similar instrumentation, but set to measure a different energy loss region, can be used to study collective (for instance, plasmons) and single particle electronic excitations.[6]

Measurement of the dynamic structure factor S($\mathbf{q}$, ω) for inelastic x-ray scattering can lead to a determination of fundamental properties of electron systems, such as the dielectric function.[7] Application of inelastic x-ray scattering to systems at high pressure can address a host of new questions about the electronic structure of matter under extreme conditions, ranging from fundamental problems of electron dynamics and correlation to chemistry, materials science, earth and planetary sciences.[8,9] The challenge for inelastic x-ray scattering measurements is the low double differential cross-section—typically orders of magnitude smaller than that of elastic scattering.

A common method to study systems at high pressure (in the GPa to Mbar range) is to use diamond anvil cells (DAC). Typical sample sizes are on the order of tens of microns. From the experimental standpoint, unwanted parasitic scattering arising from the cell can dominate the desired signal from the sample. The parasitic scattering from diamonds, gasket (which has dimensions on the order of millimeters), and pressure media can obscure the inelastic x-ray signal and prevent a clean measurement of weak inelastic scattering from the system of interest.[9,10] The problem we discuss in this paper is how to optimize the signal from the sample and minimize the parasitic inelastic x-ray scattering arising from the surrounding materials in a diamond anvil cell.

II. MINIMIZING PARASITIC SCATTERING

Because of the electron source at the advanced photon source and undulator geometry, the focused beam impinging on the sample is smaller in the vertical direction than the horizontal direction. The sample size in the axial (compression) direction of the DAC is typically 2 to 10 times smaller than in the lateral direction. Normally, the geometry is chosen so

a)pchow@carnegiescience.edu

that the DAC loading axis is vertical and perpendicular to the primary beam, so that the primary beam enters the gasket, scatters from the sample, and the scattered beam goes through the gasket on its way to the energy analyzer (Fig. 1(a)). In this way, there is a better match between the focused beam size and the sample cross-section. Selection of the focusing optics plays an important role in making a clean measurement.

Many strategies have been devised to minimize parasitic x-ray scattering from diamond anvil cells, each with its advantages and disadvantages. Receiving slits can be used to collimate the scattering from the sample region, in an attempt to cut out parasitic scattering, but effective spatial discrimination is difficult to achieve and the sample spectrum is always contaminated with contributions from diamonds and the gasket.[11] This approach requires collection of spectra from the upper and lower diamond, of the gasket as well as the sample itself. In the data reduction scheme, one finds a linear combination of the parasitic scattering, with suitable scale factors and subtracts spectra to reveal the scattering from the sample. Also, conical slits may be able to collect data more efficiently.

Internal slits can be made within the beryllium gasket (for example, alloying Be with Mo, or via laser drilling) to block the gasket scattering, but these gaskets are difficult and expensive to fabricate and sample alignment is tedious and has limited effectiveness in reducing parasitic scattering. One can eliminate the gasket scattering completely by having the primary x-ray beam enter along the axis of the diamond anvil cell, and use (partially) perforated diamonds to minimize diamond scattering and absorption of the primary beam (Fig. 1(b)). But the axial geometry limits the angular range of scattering. Moreover, the sample volume probed in the axial direction is difficult to optimize for scattering, because the sample thickness is determined by the desired pressure range. Tilting the DAC, in conjunction with recessed diamonds, may reduce the path length of x rays through the diamond and gasket (Fig. 1(c)). The use of recessed diamond limits the attainable pressures in the DAC.[12] Post-sample micro-channel arrays can be used as collimating channels,[13] but their efficiency is low due to limited solid angle of collection. Direct tomography techniques employing hard x-ray spectroscopy can image samples and provide spatial discrimination.[14] Post-sample mirrors or zone plates may give superior spatial resolution, but at the cost of reduced solid angle of collection and efficiency.

From the beam preparation standpoint, the vertical size of the beam should be well within the culet separation, with minimum tails which give rise to diamond scattering. The horizontal beam size should be smaller than the sample size

in the gasket hole. The sample size should be typically as large as possible, consistent with the pressures of interest, but constrained by its absorption length. Recent advances in DAC design can allow for relatively large sample sizes for a given pressure compared to conventional DACs.[15]

Because we are interested in the inelastic scattering energy-loss spectra, and not diffuse elastic scattering, to a certain extent, a choice can be made of the gasket material. It may be possible to select a gasket material whose inelastic spectrum has features at given $(\mathbf{q}, \omega)$ that is separated from that of the sample of interest. Instead of the typical beryllium gasket, c-BN,[16] amorphous boron/epoxy/kapton,[17] and powdered diamond gaskets can be considered. For example, diamond has an energy-loss gap of about 6 eV at intermediate scattering angles. If the excitations from the sample are within the window, there will be no parasitic scattering from diamond in that region of the spectrum.

III. POST-SAMPLE POLYCAPILLARY

Since their invention and subsequent development, Kumakhov capillary optics, also known as polycapillaries,[18–21] have been used to "channel" x rays for a variety of purposes including focusing the primary x-ray beam and post-sample collection. Polycapillaries are made from a collection of individual glass capillaries on the order of tens of microns or less in size. X-ray photons are guided along the capillary by multiple total internal reflections. The multitude of individual capillaries are arranged so that the capillaries "see" a common intersection, similar to a microscope objective, the dimension of which is called the input focal size of the polycapillary. Typical input focal sizes are on the order of tens of microns. Depending on the application required, there are several main categories of capillary optics. A half-lens polycapillary collects photons from the sample at the input focal spot and redirects the x rays into a quasi-parallel beam emerging from the exit end of the polycapillary. A focusing polycapillary refocuses the photons at its exit focal spot, after which the photons diverge. A mono-capillary is a single shaped glass tube used to focus an x-ray beam.

Using a polycapillary in confocal geometry has been employed in a number of x-ray applications, for example, in x-ray fluorescence experiments.[22–27] In some applications, two polycapillaries are used, the first which accepts x rays from a source and focuses them at the sample position. A second polycapillary collects signals only from the sample within the polycapillary's field of view and channels the scattering from the sample toward the detector. Both polycapillaries share a common focus point at the sample. These instruments employ a half-lens collimating polycapillary to collect a large solid angle of photons from the sample and map the fluorescent signal in different regions of the sample to determine spatially resolved compositions, while suppressing parasitic scattering. The micro-focus of x rays and detection spots allows for measurements of sample areas with a spatial resolution of tens of microns or less.

In this paper, we extend these ideas and describe the use of a post-sample focusing polycapillary which spatially discriminates the sample scattering from the surrounding DAC
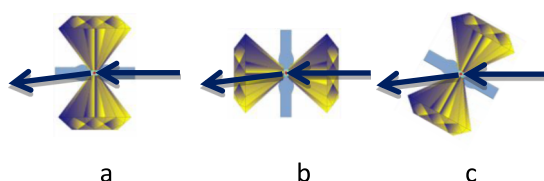

FIG. 1. Schematic view of different scattering geometries. (a) X ray enters into and exits from the gasket; (b) X-ray goes in and out from (perforated) diamonds; (c) X-ray goes in and out from a tilted DAC to reduce the path length in the gasket.

enclosing the sample, in order to reduce the parasitic scattering from the diamonds and gasket for the inelastic x-ray scattering technique. We have modified the conventionally used backscattering inelastic scattering spectrometer[28] by using a focusing polycapillary post-sample optic. We require a spectrometer with an overall energy resolution of 1.4 eV at 10 keV (which is the energy resolution of our Si(111) double crystal monochromator) to be as efficient as possible, given that the cross-section for inelastic scattering is orders of magnitude less than that of the elastic scattering.

A. Post-sample polycapillary specifications

Because a mono-capillary[29] has limited solid angle of acceptance, and a half-lens polycapillary in combination with a flat crystal analyzer has energy resolution of about 5 eV,[30] a focusing polycapillary was chosen as the post-sample optic in the inelastic x-ray scattering spectrometer.

There are a number of parameters which specify the characteristics of a focusing polycapillary. The input field of view is of primary concern. Scattering emanating from outside the input field of view is not transmitted by the polycapillary. The input field of view was specified to be slightly smaller than the sample size. The next concern is to maximize the transmission efficiency of the polycapillary (ratio of x ray intensity at exit to that entering). This is important because the small scattering cross-section even with an undulator for a 3rd generation synchrotron gives only tens of counts/s in the detector. To a certain extent, the output focal size can be specified. The output focus spot becomes the secondary "point" source for the downstream portion of the spectrometer. The output convergence angle was chosen so that only a single 4-in. diameter bent analyzer would be required to energy-analyze the scattered x rays. Finally, there is a physical constraint of being able to insert the polycapillary into the DAC at the working distance without interfering with the gasket or seats of the DAC. The remaining design parameters are free to be selected, subject to the above considerations.

As a result of optimization calculation and simulations, the following are the polycapillary specifications that were chosen:

input focal distance: 3.5 mm,

output focal distance: 60 mm,

optic enclosure diameter: 10.0 mm,

optic length: 62.5 mm,

taper input end diameter: 3.8 mm,

input collection angle: 23°,

input field of view: <20 μm FWHM at 10 keV,

output focal spot size: ~165 μm FWHM at 10 keV,

output convergent angle: ~2.5°, FWHM,

transmission efficiency: 14.8% at 10 keV.

IV. EXPERIMENTAL SET-UP

The HPCAT 16-ID-D beamline uses an APS U3.0 undulator, liquid nitrogen cooled Si (111) double crystal monochromator, 1 m long vertical and horizontal Kirkpatrick-Baez
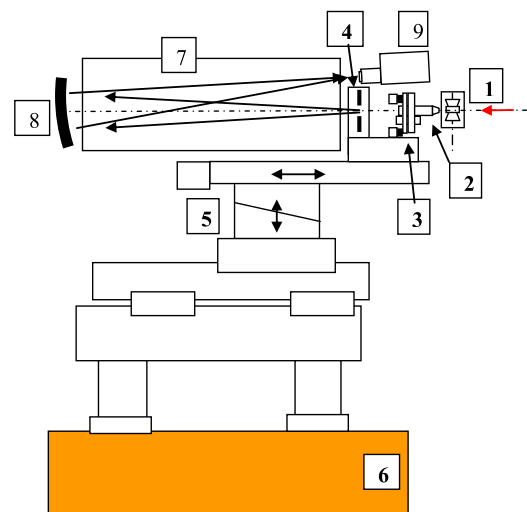

FIG. 2. Spectrometer schematic showing (1) diamond anvil cell, (2) focusing polycapillary extending into the cell, (3) in a V-block mount with tilt adjustments, (4) slit at output focus position of the polycapillary, (5) XYZ positioners with micron stability and repeatable motion, (6) 2θ arm to select the scattering angle, (7) helium flight path, (8) single 4-in. bent Si (111) analyzer, (9) Si detector in backscattering geometry with 87.15° Bragg angle.

mirrors to focus 9.886 keV x rays to 30 μm (vertical) × 60 μm (horizontal) at FWHM. A single 100 mm diameter Si(555) bent analyzer was used to energy-analyze the scattered beam. An Amptek XR 100CR Si-PIN detector was positioned directly over the DAC in near backscattering geometry at 87.15° Bragg angle. Figure 2 shows a schematic of the spectrometer. Figure 3 shows a photo of the focusing polycapillary in use for a measurement.

A. Alignment of the polycapillary and inelastic x-ray scattering spectrometer

The spectrometer without polycapillary was pre-aligned so that elastic scattering from a glass fiber at the sample
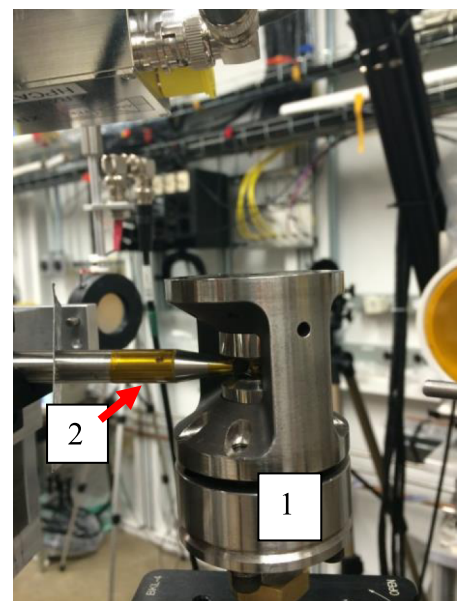

FIG. 3. Photo showing the focusing polycapillary (2) extending into the DAC (1).

position is diffracted by the analyzer, and collected by the detector in backscattering geometry. The polycapillary was then aligned as follows. We sought to align the polycapillary so that the central axis of the polycapillary intersects the sample position (radially from the sample position), the axis is in the scattering plane of the spectrometer, and the input end of the polycapillary is at the input focal distance from the sample position. The polycapillary is mounted on a V-block holder with two manual tilt adjustments (the polycapillary is axially symmetric) and three motorized positioners (radially from the sample position, transverse to the polycapillary axis, and vertically) with precision and stability of about 1-2 μm. The translation stage which moves the polycapillary radially from the sample position needs to have a long enough travel to back out the polycapillary to align the sample in the DAC.

It is important to pre-align the V-block holder to set the two tilting angles of the polycapillary. By construction, the polycapillary axis is aligned in the cylindrical housing within 0.1°. To align the tilt angles, we rotate the spectrometer arm to zero scattering angle (so that the x-ray main beam would be nominally going down the axis of the polycapillary), and with the main beam, take an x-ray burn upstream and downstream of the V-block mount. With an auxiliary double-ended pointer in the V-block, we adjust the tilt angles so that the pointer tips coincide with the burn marks. This tilting adjustment procedure will adequately align the polycapillary axis radially from the sample position, and put the polycapillary axis in the scattering plane.

Next, we use a dummy pointer which has the same dimensions as the polycapillary except extended to a point at the input focal distance. After taking an x-ray burn at the sample position, we adjust the 3 motorized positioners to roughly position the dummy pointer better than 100 μm visually. We then mount the polycapillary in the pre-aligned V-block. This completes the polycapillary pre-alignment procedure.

Continuing with the spectrometer alignment, we use the fluorescence from a nickel wire 100 μm diameter in the main beam at a scattering angle of 40° as the point source of scattering to fine position the polycapillary. After mounting the polycapillary at about the correct input focal distance, we back out the positioned polycapillary a few millimeters greater than the input focal distance, translating it radially away from the sample position. The area which the polycapillary "sees" is then larger to make it easier for initial alignment with Ni fluorescence. A Pilatus 100 K area detector, about 1 m from the sample position, is employed to look at the image of the photons coming out of the polycapillary to assist in alignment.

Scanning the polycapillary vertically and transverse should produce an image from the polycapillary in the Pilatus, which is continuously displaying images. Transverse and vertical scans using the integrated Pilatus signal are iterated as the polycapillary is stepped closer to the sample position. The polycapillary is at the optimum input focal distance when the peaks in the transverse and vertical scans are maximum and the widths of the peaks are the size of the designed input field of view.

After the polycapillary is aligned, a slit is placed at the polycapillary exit focus distance. The pre-aligned Amptek Si detector is moved downstream to be vertically above the
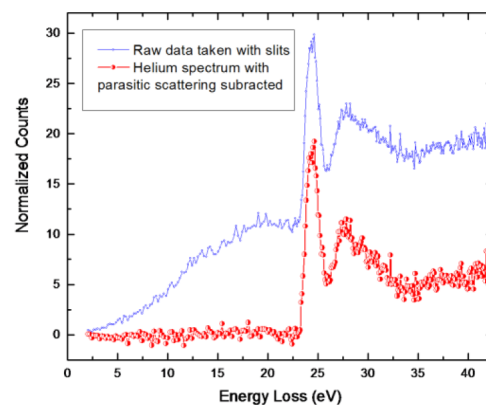

FIG. 4. Combined raw data from several scans taken with conventional post-sample slits used to reduce parasitic scattering from the DAC, along with analyzed data after the parasitic scattering from diamond and the gasket were subtracted. Typical count rate in the main peak of the background subtracted helium spectrum was 220 cts/min.

slit at the polycapillary exit focus. The analyzer is translated downstream, and the entire spectrometer alignment is fine-tuned.

V. RESULTS

Figure 4 shows the spectrum of helium measured in a panoramic DAC at 13.4 GPa using conventional receiving slits (250 μm wide, 3 mm tall slot approximately 3.0 mm from the sample) and a 17-element analyzer array at 40° scattering angle. The analyzer array consists of 17 two-inch diameter bent Si(111) wafers arranged in three columns, which focus analyzed x-ray photon into the detector. There is significant contamination of the helium scattering from the diamonds and the gasket in the raw data as measured. After positioning the DAC to measure the upper and lower diamonds and the beryllium gasket, the best estimate of the parasitic scattering was subtracted from the raw spectrum, revealing the helium spectrum.

For comparison, using the focusing polycapillary and a single bent Si(111) analyzer, the corresponding raw data from single scan shows the helium spectrum, Figure 5, with significantly reduced diamond and gasket scattering.

Scattering from beryllium at this scattering angle would give rise to continuous scattering starting from the elastic line. The diamond would have a gap in energy loss of about 5 eV and then contribute to the parasitic scattering. Neither the Be nor diamond contributions are evident in the raw spectrum using the polycapillary. The data taken with polycapillary as a post sample optic have a signal-to-background ratio ~15:1, compared to just ~2:1 using a conventional slit. This demonstrates the effectiveness of using the focusing polycapillary post-sample optic.

The data using slits versus the polycapillary post-sample optic were taken with different beam line conditions. The polycapillary accepts scattering from a full cone angle of 23°, whereas the slits accepted just 0.3 mm^2 at 3.5 mm from the sample. The spectra cannot be directly compared because different ranges of momentum transfer are measured. We
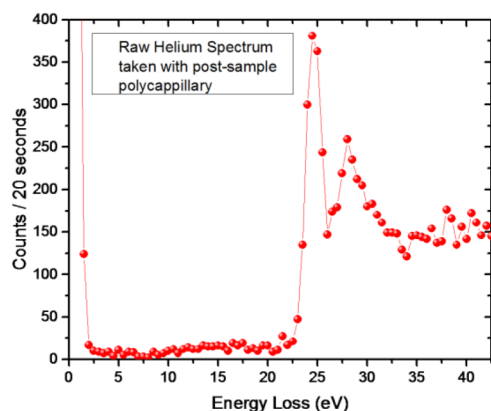
FIG. 5. Raw data (no data processing) taken in a DAC in a single scan of 20 s/pt with the focusing polycapillary as the post-sample optic. The large scattering near zero energy loss is the tail of the elastic line. There is an excitation gap ranging from about 2 to 23 eV, a sharp exciton peak close to 25 eV and the continuum excitation spectrum of helium.

sought to understand all the factors which contribute to the measured count rate. When we compared the raw data for each case, taking into account the relative incident photons/s in the focused beam on the sample, the sample sizes and densities, the collection area of the slits compared to the solid angle accepted by the polycapillary, the polycapillary transmission efficiency, and the efficiency of the different analyzer configurations, the estimated count rate in the peak of the helium exciton was within 15% of the measured count rate. The essential difference in the measured spectra is of course the large parasitic scattering using slits, compared to the cleaner spectrum using the polycapillary post-sample optic. Considering scattering in the horizontal plane, the polycapillary field of view is 20 μm and the sample size was 150 μm, so even with the projection at the scattering angle of 40° the polycapillary allows only scattering from the helium sample to be transmitted to the analyzer, as long as the beam focus size is smaller than the sample size. By contrast, the slit configuration allows an estimated 0.7 mm of illuminated path length through the beryllium gasket to go to the analyzer while allowing the 150 μm path length of the beam through the helium sample to be measured. In the vertical plane, the contribution to the measured spectrum from the diamond scattering is due to the size of the focused beam relative to the culet separation. In the case of the polycapillary post-sample optic, the polycapillary does not collect the diamond scattering when its field of view is smaller than the sample thickness.

VI. DISCUSSION AND CONCLUSIONS

For the measurement described in this paper, the use of a post-sample polycapillary significantly reduces parasitic scattering, because the polycapillary "sees" predominantly the sample volume. Scattering originating from the gasket and diamonds is outside the field of view of the polycapillary and is not transmitted. At larger scattering angles, the polycapillary "sees" less of the projection of the primary beam through the gasket, so the effectiveness of rejecting parasitic scattering improves. At lower scattering angles and for higher pressures,

where the sample size gets smaller, the polycapillary will not have an effective spatial discrimination. The input focal size is governed by the density of the polycapillary material, the energy of the x rays, the alignment of the individual capillaries, and the distance of the sample from the input end of the polycapillary. For the polycapillary designed and fabricated for this measurement, to a reasonable approximation, the focal size is estimated to be

$$\text{input focal size} \approx 2\,\theta_c * (\text{input focal distance}),$$

where the critical angle for total reflection θ_c (mrad) is 30/(photon energy in (keV)) for borosilicate glass. The critical angle is proportional to the square root of the capillary material density. Borosilicate glass is chosen because its properties are suitable for fabrication, and for its relatively low density, which leads to a small critical angle. 10 keV x ray was chosen to maximize the incoming primary beam intensity, and also to give 1.4 eV overall energy resolution appropriate for the measurement of the helium excitations. The post-sample polycapillary did not degrade the energy resolution of the spectrometer. Using higher energy x rays to resolve finer features, for example, corresponding to higher energy resolution Si(777) leads to a smaller critical angle, and a small input focal size, at the expense of transmission efficiency.

In a diamond anvil cell, the diamond seats can limit how close the polycapillary can be to the sample. Beryllium gasket sizes are typically 3–5 mm diameter. Polycapillary housings and DAC designs can be optimized so that the polycapillary can be positioned as close to the sample as possible.

As a rule of thumb, the beam size and input focal size should be smaller than the sample size due to the tails of the primary beam. Even with a well-focused primary beam the tails illuminate the gasket and diamond, which have relatively large scattering volumes and cross-sections compared to the sample. The polycapillary used in this measurement was axially symmetric, producing a circular input focal spot. Polycapillaries with elliptical input focal spots can take advantage of the sample shape within a DAC and focused beam cross-section, in which the axial sample dimension is generally smaller than the transverse dimension.

The effective collection solid angle of the polycapillary is limited by the required output divergent angle. The performance of the polycapillary used in this experiment was already approximately 50% of the theoretical performance. To further enhance the data collection beyond the single-optic approach, several polycapillaries can be multiplexed to form a multichannel spectrometer. Another limitation of the polycapillary in the way it was used is the loss of determination of the **q**-dependence of the inelastic scattering. The measured signal was the integration of the inelastic scattering within the polycapillary input solid angle. In this work, the input solid angle of the polycapillary is 23° and the 2θ arm was set at 40°, so scattering from 28.5° to 51.5° was collected which corresponded to a large range of q. However, the polycapillary can be used as an imaging optic. Techniques have been developed to extract the angle-dependence of the scattering using a post-sample polycapillary for q-dependent data collection. We are presently applying this technique to measure the electronic excitations of other systems.

As mentioned above, the transmission efficiency of the polycapillary used in this work at 10 keV is ~15%. Due to signal intensity loss of ~6 times compared to a conventional slit, this technique is useful to measure excitations close to the elastic peak energy (a few eV to tens of eV) where background scattering from gasket and diamonds of DAC dominate. However, for x-ray Raman scattering experiments for which excitations are hundreds of eV away (C, N, and O), parasitic scattering is less dominant and the signal is much less due to smaller scattering cross-section for low Z materials. It is difficult to compensate the loss of signal through the polycapillary.

Recent advances in instrumentation (such as capillary optics and area detectors) to x-ray spectroscopy are limited only by the creativity of the experimenter. In summary, parasitic scattering from gasket and diamonds of a DAC obscure the weak inelastic scattering signal from the sample of interest. We have designed and built an inelastic x-ray scattering spectrometer using a focusing polycapillary as a post-sample optic. In the measurement of the inelastic scattering spectrum of helium at high pressure, the use of a post-sample polycapillary significantly reduced the parasitic scattering from the diamond anvil cell.

ACKNOWLEDGMENTS

[1]W. Schulke, H. Nagasawa, S. Mourikis, and A. Kaprolat, Phys. Rev. B **40**, 12215 (1989).

[2]W. Schulke, H. Schulteschrepping, and J. R. Schmitz, Phys. Rev. B **47**, 12426 (1993).

[3]W. Schulke, H. Nagasawa, and S. Mourikis, Phys. Rev. Lett. **52**, 2065 (1984).

[4]W. A. Caliebe, J. A. Soininen, E. L. Shirley, C. C. Kao, and K. Hamalainen, Phys. Rev. Lett. **84**, 3907 (2000).

[5]Y. Mizuno and Y. Ohmura, J. Phys. Soc. Jpn. **22**, 445 (1967).

[6]W. Schülke, *Electron Dynamics by Inelastic X-ray Scattering* (Oxford University Press, 2007).

[7]K. Sturm, Z. Naturforsch., A: Phys. Sci. **48**, 406 (1993).

[8]H. K. Mao, C. C. Kao, and R. J. Hemley, J. Phys.: Condens. Matter **13**, 7847 (2001).

[9]J.-P. Rueff and A. Shukla, Rev. Mod. Phys. **82**, 847 (2010).

[10]D. Yang, C. Cheng-Chien, Z. Qiaoshi, K. Heung-Sik, H. Myung Joon, M. Balasubramanian, R. Gordon, L. Fangfei, B. Ligang, D. Popov, S. M. Heald, T. Gog, M. Ho-kwang, and M. van Veenendaal, Phys. Rev. Lett. **112**, 056401 (2014).

[11]M. Ho Kwang, E. L. Shirley, D. Yang, P. Eng, Y. Q. Cai, P. Chow, X. Yuming, S. Jinfu, R. J. Hemley, K. Chichang, and W. L. Mao, Phys. Rev. Lett. **105**, 186404 (2010).

[12]R. A. Mayanovic, A. J. Anderson, W. A. Bassett, and I. M. Chou, Rev. Sci. Instrum. **78**, 053904 (2007).

[13]A. R. Woll, D. Agyeman-Budu, D. H. Bilderback, D. Dale, A. Y. Kazimirov, M. Pfeifer, T. Plautz, T. Szebenyi, and G. Untracht, Proc. SPIE **8502**, 85020K (2012).

[14]S. Huotari, T. Pylkkanen, R. Verbeni, G. Monaco, and K. Hamalainen, Nat. Mater. **10**, 489 (2011).

[15]R. Boehler, M. Guthrie, J. J. Molaison, A. M. dos Santos, S. Sinogeikin, S. Machida, N. Pradhan, and C. A. Tulk, High Pressure Res. **33**, 546 (2013).

[16]W. Lin, Y. Wenge, X. Yuming, L. Bingbing, P. Chow, S. Guoyin, W. L. Mao, and M. Ho-kwang, Rev. Sci. Instrum. **82**, 073902 (2011).

[17]J. F. Lin, J. Shu, H. K. Mao, R. J. Hemley, and G. Shen, Rev. Sci. Instrum. **74**, 4732 (2003).

[18]N. Gao and I. Y. Ponomarev, X-Ray Spectrom. **32**, 186 (2003).

[19]C. A. MacDonald, X-Ray Opt. Instrum. **2010**, 1.

[20]C. A. Macdonald, J. X-Ray Sci. Technol. **6**, 32 (1996).

[21]D. H. Bilderback, X-Ray Spectrom. **32**, 195 (2003).

[22]S. Heald, G. T. Seidler, D. Mortensen, B. Mattern, J. A. Bradley, N. Hess, and M. Bowden, Proc. SPIE **8502**, 850201 (2012).

[23]S. V. Nikitina, A. S. Shcherbakov, and N. S. Ibraimov, Rev. Sci. Instrum. **70**, 2950 (1999).

[24]S. Smolek, C. Streli, N. Zoeger, and P. Wobrauschek, Rev. Sci. Instrum. **81**, 053707 (2010).

[25]M. Wilke, K. Appel, L. Vincze, C. Schmidt, M. Borchert, and S. Pascarelli, J. Synchrotron Radiat. **17**, 571 (2010).

[26]N. Gao, I. Y. Ponomarev, Q. F. Xiao, W. M. Gibson, and D. A. Carpenter, Appl. Phys. Lett. **71**, 3441 (1997).

[27]A. Bjeoumikhov, N. Langhoff, S. Bjeoumikhova, and R. Wedell, Rev. Sci. Instrum. **76**, 063115 (2005).

[28]D. Sokaras, D. Nordlund, T. C. Weng, R. A. Mori, P. Velikov, D. Wenger, A. Garachtchenko, M. George, V. Borzenets, B. Johnson, Q. Qian, T. Rabedeau, and U. Bergmann, Rev. Sci. Instrum. **83**, 043112 (2012).

[29]R. Huang and D. H. Bilderback, J. Synchrotron Radiat. **13**, 74 (2006).

[30]D. R. Mortensen, G. T. Seidler, J. A. Bradley, M. J. Lipp, W. J. Evans, P. Chow, Y. M. Xiao, G. Boman, and M. E. Bowden, Rev. Sci. Instrum. **84**, 083908 (2013).